Investigating Spectra of Spiking Behavior in Area 5 of the Parietal Cortex

by

Keith Dyson

A Thesis Presented in Partial Fulfillment
of the Requirements for the Degree
Master of Science

Approved April 2013 by the
Graduate Supervisory Committee:

Christopher Buneo, Chair
Marco Santello
Stephen Helms Tillery

ARIZONA STATE UNIVERSITY

May 2013

ABSTRACT

In order to successfully implement a neural prosthetic system, it is necessary to understand the control of limb movements and the representation of body position in the nervous system. As this development process continues, it is becoming increasingly important to understand the way multiple sensory modalities are used in limb representation. In a previous study, Shi et al. (2013) examined the multimodal basis of limb position in the superior parietal lobule (SPL) as monkeys reached to and held their arm at various target locations in a frontal plane. Visual feedback was withheld in half the trials, though non-visual (i.e. somatic) feedback was available in all trials. Previous analysis showed that some of the neurons were tuned to limb position and that some neurons had their response modulated by the presence or absence of visual feedback. This modulation manifested in decreases in firing rate variability in the vision condition as compared to nonvision. The decreases in firing rate variability, as shown through decreases in both the Fano factor of spike counts and the coefficient of variation of the inter-spike intervals, suggested that changes were taking place in both trial-by-trial and intra-trial variability. I sought to further probe the source of the change in intra-trial variability through spectral analysis. It was hypothesized that the presence of temporal structure in the vision condition would account for a regularity in firing that would have decreased intra-trial variability. While no peaks were apparent in the spectra, differences in spectral power between visual conditions were found. These differences are suggestive of unique temporal spiking patterns at the individual neuron level that may be influential at the population level.

TABLE OF CONTENTS

LIST OF FIGURES

Chapter 1

INTRODUCTION

Neural engineering is a young field, emerging at the intersection of neuroscience and biomedical engineering. Applications of engineering approaches and quantitative methodology to problems in neuroscience differentiate neural engineering from other, established fields, such as neurophysiology. Neural engineers are using experimental, theoretical, computational, and clinical approaches to solution of neuroscience problems at the molecular, cellular, and systems levels (Durand, 2006).

There is a wealth of applications for the fruits of neural engineering research. This research can lead to better understanding of healthy neural activity and tissue, which can in turn, lead to better understanding of damages and impairments to the nervous system. This understanding can be leveraged toward the development of effective rehabilitation techniques for patients with stroke, traumatic brain injury, or any of a number of other neurological conditions. Furthermore, a deeper understanding of the way neural signals govern global behavior can lead to the development of neural prostheses or a brain-machine interface. In order to do this, it is necessary to implement a system that records the neural signals, decodes the commands carried by these signals, and uses it as a control signal for an external device, such as a robotic arm or a computer cursor. Such a system could be very beneficial to an amputee or paralyzed person.

In fact, over the last 50 years, a remarkable amount of progress has been made toward the development of functioning neural prosthetics and brain-machine interfaces (BMI). One of the first BMIs to be implemented was the cochlear implant in 1958, by French surgeons Andre Djourno and Charles Eyries (Eisen, 2003). In 1980, Dr. Edward Schmidt first proposed that a neuroprosthetic device could be used to restore motor

function to patients with severe paralysis (Nicolelis, 2003). Since its first suggestion, work in the field has continued for decades, to the extent that clinical trials are currently underway for chronically implanted electrodes that allow paralyzed users to control an external robotic arm in order to regain lost motor function (Hochberg et al., 2006).

While the progress being made towards achieving a functional robotic neurally-controlled prosthesis is exciting and groundbreaking, the current approaches suffer from a few important limitations. Glial encapsulation of chronically implanted electrodes threatens to degrade signal integrity over time (Polikov, Tresco, & Reichert, 2005). Sparsity of sampling from the thousands of neurons involved in motor control creates challenges in decoding the entire command from a portion of the signal (Li, Smith, Hargrove, Weber, & Loeb, 2013). But one of the most fundamental issues with the current approach is that the user of the device is not receiving the same kind of feedback from the prosthetic device that a healthy person receives from his or her own limb (Schwartz et al., 2006).

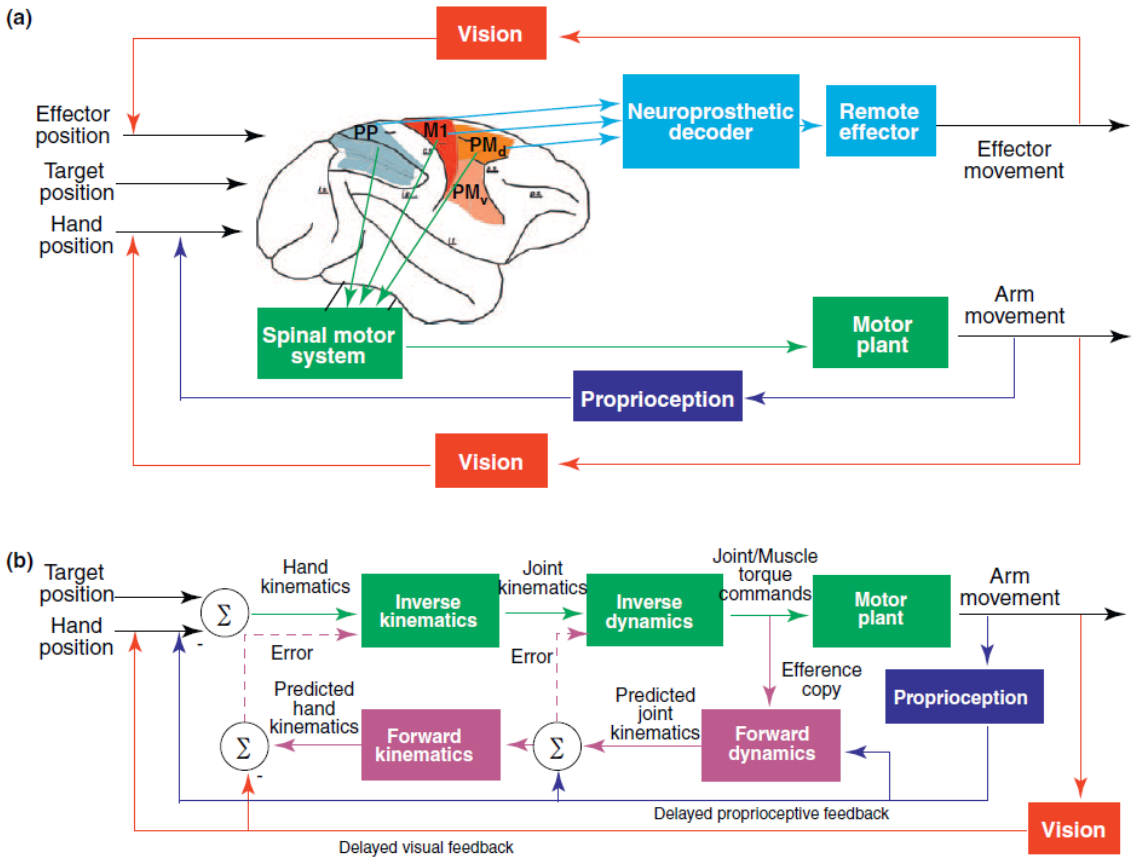

Figure 1 Schematic of Control Systems and Block Diagram (Green and Kalaska, 2011)

In a healthy person, data on limb position and movement is provided through a few channels. The bottom of Figure 1A shows a simple set up of the system – motor commands generated in relevant cortical areas descend through spinal motor system pathways to the motor plant, where they are transformed into arm movements. Feedback to the system can be relayed to the central nervous system (CNS) through two routes. First and most obvious is visual information. Vision of the limb in space can be used by the nervous system in the planning and execution of movements. The second route, somatic information, comes from two sources: efference copy and proprioception. Figure 1B shows an illustration of the system thought to be used in the control of arm movements. The movement vector is calculated as the difference between hand and target position. Then, the hand kinematics required to achieve the vector are calculated, followed by the arm joint kinematics required

to achieve the desired hand kinematics to move to the target. The joint kinematics are translated into a set of joint and muscle torque commands which are relayed to the motor plant for execution of the planned movement. These commands are fed back into the system as what is known as "efference copy". Provision of efference copy allows the system to make predictions of the effects of motor commands and estimate limb position based on the previous commands. Proprioception, which is the sense that allows an individual to know the position of his/her limb even in the absence of vision, is provided to the CNS by the Golgi tendon organs and muscle spindles. In this document, proprioception and efference copy are grouped together as "somatic feedback" and are distinguished from visual feedback.

The top section of Figure 1A shows the same system as the bottom section, but for a BMI implementation. While a neural prosthetic device is obviously capable of being seen by the user and can therefore be accounted for by the visual feedback system, current neural prosthetic systems do not incorporate somatosensory feedback. Because the CNS is typically able to integrate data from multiple sensory modalities, a neural prosthesis with a unimodal (vision only) source of sensory feedback will not provide a full set of sensory data. As neural prosthetic systems become more advanced, this deficit of somatosensory data is becoming more pronounced and more necessary to correct (Schwartz et al., 2006). One way to do this is to provide stimulation into the nervous system in lieu of natural somatosensation. However, before artificial sensation can be effectively implemented, it will be important to fully understand the roles of the different types of sensory data in the sensorimotor integration process.

In studying neural activity in response to a stimulus, there are many characteristics of activity which are important to characterize in order to obtain a clear picture of the neural

behavior. Most obviously, the mean firing rate can show changes in activity – an overall increase or decrease in activity that occurs with stimulus onset (or offset) can indicate that the neuron is responding to the stimulus via excitation or suppression (respectively). However, as demonstrated by Churchland et al. (2010), even neurons that do not exhibit a change in mean firing rate can exhibit changes in neural variability in response to a stimulus. In fact, Churchland et al. (2010) showed that in a wide range of cortical areas neural variability decreases with stimulus onset (provided that the neuron in question is part of a network that responds to the stimulus in question).

Two statistical measures frequently used in studying the variability of neural activity are the Fano factor (FF) of the spike count and the square of the coefficient of variation (CV) of the inter-spike interval (Nawrot et al., 2008). Both FF and CV are normalized measures of the variance that control for the mean rate. The FF, which uses spike counts for each trial, helps to quantify trial-by-trial variability. The CV, using the inter-spike interval, measures the intra-trial variability. Assessing both trial-by-trial and intra-trial variability and comparing the two measures of variability between conditions can provide insight into the neural coding of both sensory and motor variables.

In addition to the Fano factor and the coefficient of variation, an important tool for describing the variance of a signal is the frequency spectrum. While it is easy to comprehend and visualize a signal in the time domain – it is simply a series of points representing the value of the signal at each time point – visualizing the same signal in the frequency domain can be somewhat more intuitively challenging. A key idea allowing time signals to be represented in the frequency domain is that any periodic signal can be decomposed and represented as a sum of elementary periodic signals (sine and cosine functions or complex exponentials). This idea is known as Fourier's theorem, and the process of transforming a

function from its representation in the time domain to its frequency domain counterpart is called the Fourier transform (Maor, 2002). By taking the average magnitude squared of the Fourier transform, one obtains the periodogram of a time signal, which provides us with an estimate of its spectral density (Percival & Walden, 1993).

In order to help conceptualize the spectrum, Figure 2 (from Jarvis & Mitra, 2001) provides spectra for three different hypothetical processes. In (A), a spectrum is provided for a completely homogeneous Poisson process. The spectrum is constant for all frequencies at the value λ, which is the mean firing rate for the process. The second example, (B), shows a spectrum for a process with regular spiking interval ΔT with a small amount of drift. The spectrum is defined by sharp peaks at frequencies that are multiples of $\frac{1}{\Delta T}$. The addition of drift causes a blur to occur at higher frequencies and it stabilizes to λ at high frequencies. In (C), a spectrum is shown for a process in which the probability of the next spike is suppressed immediately following a given spike, consistent with a refractory period. The spectrum is suppressed at low frequencies, but goes to the constant λ at high frequencies.

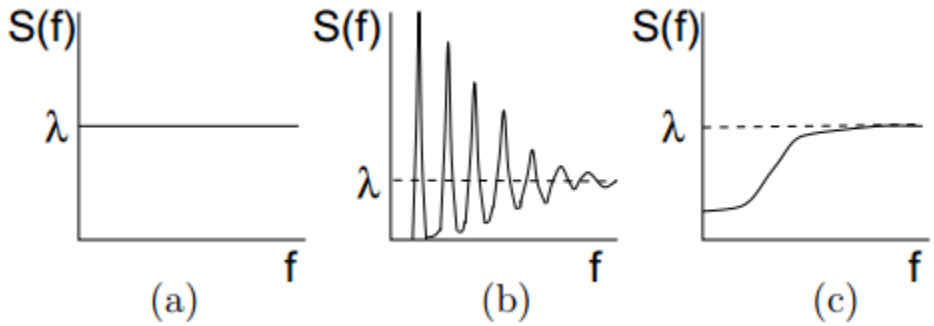

Figure 2 Sample spectra (a) shows a completely homogeneous Poisson process, (b) shows a process with regularly spaced spikes with jitter, and (c) shows a Poisson process with suppression at low frequencies. (Jarvis & Mitra, 2001).

The spectrum can provide us with a fuller understanding of the variation of the signal, since the spectral value at a given frequency is representative of the amount of variation in the signal accounted for by the frequency in question. Spectral analysis is

frequently used in the study of continuous processes (such as the local field potential, or LFP) but can also be used to analyze point processes. Because action potential spikes are considered to be a uniform, binary occurrence – either a spike occurred or it did not – a train of spikes can be represented as simply a list of the times at which they occurred (Buneo et al., 2003). This data can easily be used to calculate the CV and FF, using the spike counts for each trial and the time interval between spikes (the inter-spike interval), but can also be used to create a frequency spectrum, which is then used for spectral analysis. This is done using the autocovariance of the process, which shows how similar a function is to itself at given time lags. In other words, given that a spike occurred at time T, how likely is it that a spike will occur at time T + τ, where τ is the time lag.

Recently, in an effort to understand the roles of different sensory modalities underlying limb representation, rhesus monkeys were trained to perform a simple reaching task from a center starting point to one of eight target positions arranged radially around the starting point (Shi et al., 2013). After the monkey performed a successful reach to the target, he made a saccade back to the starting position while fixating his hand at the target position and held this position for a set holding period (see further description in Methods). In some trials, the monkey was provided visual feedback of his hand during the holding period, while in others, he was not. In so doing, comparisons can be made between the activity in trials when the monkey was provided with multimodal sensory data (vision + somatic) with trials when the monkey was only provided with unimodal sensory data (somatic). By characterizing the differences between the conditions, it is possible to expand the understanding of the roles of different sensory modalities in creating a limb representation in the brain.

Initially, the analysis has been limited to characterization of the variance through use of the Fano factor and the coefficient of variation. Using these measures, it was found that FF and CV were larger in the non-vision conditions, as compared to vision (Shi et al., 2013). However, this is still an incomplete characterization of the variance – and one that does not explain the origin of the differences between conditions. In particular, it is unclear what is causing the changes in intra-trial variability. A lower CV of the inter-spike interval in trials with visual feedback suggests that perhaps vision is stabilizing the system, creating more regularity in the ISI. This effect could be seen in the temporal structure of the neural spiking behavior. In order to further understand the nature of the variance and differences between conditions, I calculated spectra for all of the recorded cells. This spectral analysis was expected to show differences in temporal structure between the two conditions, which may help to understand the differences in variance between them as well.

Chapter 2

METHODS

Experimental Apparatus

Two head-fixed animals (monkey X, monkey B; Macaca Mulatta) were trained to make arm movements using visual feedback provided by a computer-generated, 3D virtual environment. A schematic is shown in Figure 3. Though vision of the animal's arm was blocked, wrist position was shown as a green sphere displayed by a 3D monitor (Dimension Technologies, Inc.) that projected onto a mirror on the surface that blocked vision of the arm from the animal. Arm movements were monitored using an active LED-based motion tracking system (Phoenix Technologies Inc, sampling rate: 250 Hz, spatial resolution: 0.015mm at 1.2m distance). A remote optical eye tracking system (Applied Science Laboratories Inc., sampling rate: 120 Hz, spatial resolution: 0.25 degrees of visual angle) was used to monitor eye movements.

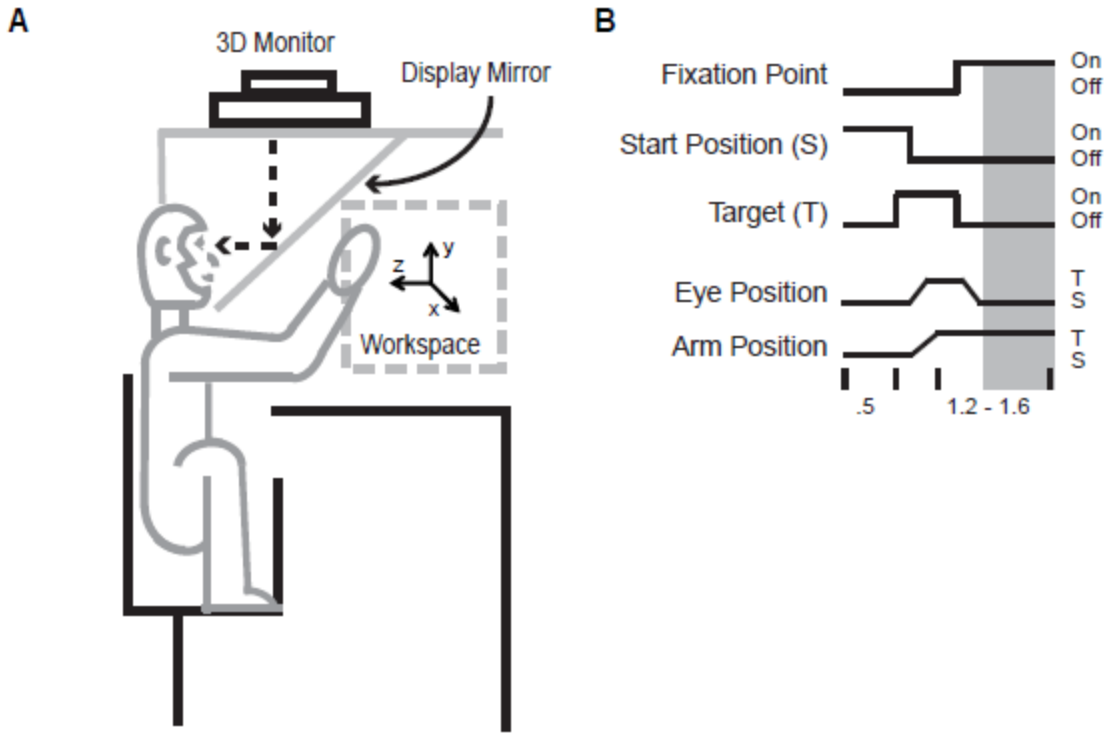

Figure 3 Experimental Apparatus and Paradigm (A) Schematic of virtual reality set up. (B) Sequence of events of a single trial. Grey rectangle denotes static holding period that was the focus of this study.

Experimental Paradigm

Animals performed a reaction-time task that combined eye and arm movements from a single starting position in the center of the workspace to one of eight peripheral targets, which were followed by a saccadic eye movement back to the central fixation point (Fig. 3) (Shi et al, 2013). At the start of each trial, the starting position was presented, represented by a green sphere in the center of the visual workspace. After the animal moved his arm to the start position, he was required to maintain the position for 500 ms, at which point a second target was presented at one of 8 locations arranged in a rectangle (monkey X) or square (monkey B) in a frontal plane. After being presented with the target sphere, the animal moved its arm to the target. For monkey X, targets were separated by 5 cm along the horizontal axis and 4 cm along the vertical axis and were therefore up to 6.4 cm from the center of the workspace. For monkey B, targets were separated by 5 cm along both

horizontal and vertical axes and were therefore 7.1 cm from the center of the workspace (Shi et al., 2013).

A green sphere representing hand position was displayed to the animal at the beginning of each trial and throughout the movement toward the target. After acquisition of the reach target by the animal, the target was extinguished after 300 ms (monkey X) or 400 ms (monkey B). A yellow sphere was then presented at the center of the visual workspace, where the animal was required to fix his vision. After making a saccade to the yellow target sphere, a 'static holding period' began, during which the animals continued to fixate vision at the center of the display while also maintaining arm position at the peripheral target for a period of 800 ms. During this static holding period, visual feedback of hand position was provided on half of the trials (Visual condition (V)) but was withheld on the remaining trials (No Vision Condition (NV)). Data analysis focused on the 800 ms of the static holding period (Shi et al, 2013).

Spherical windows with radius 2cm (monkey X) or 2.4 cm (monkey B) surrounded each reach target and a behavioral window of radius ~6.5 of visual angle surrounded the central visual fixation point. In order to successfully complete a trial, the animal was required to maintain position within these windows throughout the holding period. Five (5) trials were performed for each target, which were pseudorandomly selected (Shi et al., 2013).

Neurophysiology

All experimental procedures were conducted according to the "Principles of laboratory animal care" (NIH publication no. 86-23, revised 1985) and were approved by the Arizona State University Institutional Animal Care and Use Committee. Single cell recordings (N=343; 219 from monkey X and 124 from monkey B) were made in in the

superficial cortex of the superior parietal lobule (area 5), which was judged by recording depth and similarity to previous recordings made in this area (Buneo et al. 2008; Buneo et al 2002; 2003), using standard neurophysiological techniques. Spiking activity was recorded extracellularly with varnish-coated tungsten microelectrodes (~1-2M impedance at 1 kHz). Single action potentials (spikes) were isolated from the amplified and filtered (600-6000 Hz) signal through use of a time-amplitude window discriminator (Plexon Inc.). Spike times were sampled at 2.5 kHz (Shi et al, 2013).

Data Analysis

Single cell and population spectra were calculated from activity recorded during the static holding period of the task – only spikes occurring in the 800 ms window after the monkey fixated on the central fixation point were used. Because the rate of neural spiking activity is approximately constant during this period, it can be reasonably assumed that the process is stationary. A sequence of spike arrival times $\{t_j\}$, j = 1…N is recorded on the interval [0,T]. The first step in evaluating the spectrum is to take the square of the modulus of the Fourier transform of the data:

$$S^D(f) = \frac{\left|\sum_{j=1}^{N} e^{-2\pi i f t_j} - N\right|^2}{T}$$

Subtracting N removes the mean from the data (Jarvis and Mitra, 2001). Next, the result is smoothed using a Gaussian kernel, which reduces its variance:

$$S^{LW}(f) = \int_{-\infty}^{\infty} K(f - f')S^D(f')df'$$

This estimate is known as a lag window spectral estimator (Jarvis and Mitra, 2001). Spectral estimates were averaged over all trials for each cell in each direction in both conditions.

Using a 2-factor analysis of variance (ANOVA) on the mean firing rate with limb position and visual condition as the factors ($p<0.05$), spectral data for cells was sorted by

response to vision only (VO), position only (PO) and the position-vision interaction (PV) and by preferred direction for each cell (Shi et al, 2013). Population averages and 95% confidence intervals for both V and NV conditions were created using a bootstrap distribution with 1000 resamples. For PO, VO, and PV populations, comparisons between V and NV conditions were made in low frequency band (0-10 Hz) and gamma band 30-100 Hz) using a permutation test with 1000 samples.

Chapter 3

RESULTS

Of 343 cells recorded, 39% (135) showed statistically significant response to limb position during the 800 ms static holding period, 13% (44) showed significant main effect of vision, and 9% (27) exhibited interaction effects of position and vision (main and/or interaction effects; ANOVA, $p<0.05$). In all, 44% of neurons showed some effect of position (i.e. had main and/or interaction effects) and 19% demonstrated either main or interaction effects of vision. Eleven (11) percent of neurons demonstrated effects of both position and vision. The neuron shown in Fig. 4 below is representative of the majority of neurons recorded in the study. Shown are spike rasters and peristimulus time histograms for the neuron. The cell responded similarly in both V and NV trials. ANOVA on mean firing rate during the static holding period showed a main effect of position ($p<0.05$) with no effect of visual condition ($p=0.52$) and no interaction effect ($p=0.64$). Because the cell responded to limb position regardless of visual condition, the cell appeared to encode limb position using only somatosensory data.

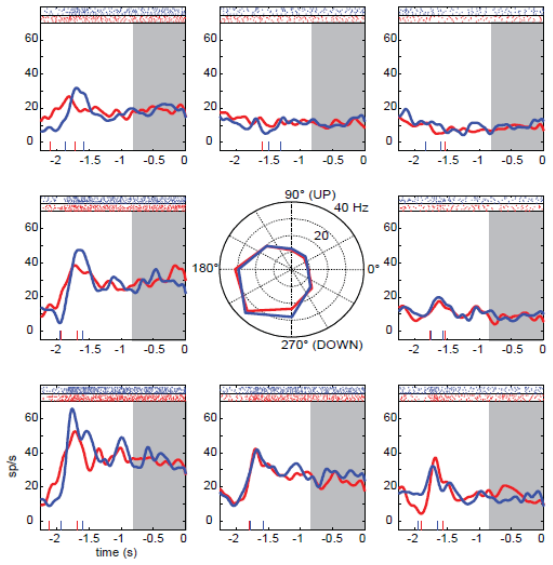

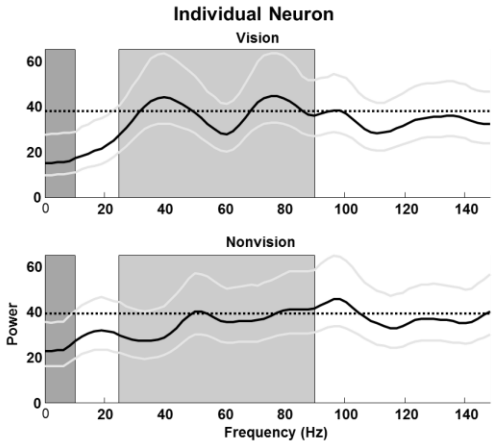

Figure 4 (left): Peristimulus Time Histogram for an individual neuron. Activity of single neuron aligned to the end of the static holding period. Center shows a polar plot of mean activity during analysis window (grey rectangle). Preferred direction for this neuron was 225 degrees (bottom left). (Shi et al., 2013)

Figure 5 (right) Calculated spectra for same individual neuron shown in Figure 4. Black line represents spectrum, gray lines represent 95% confidence interval. Dotted line represents λ for process. Low frequency and gamma bands are shown with large gray rectangles.

Figure 5 shows the spectra calculated for the same neuron shown in Figure 4 for the neuron's preferred direction (225°, lower left box of Figure 4) in both V and NV conditions. Spikes occurring in the gray rectangle on the right of each subplot were used in the construction of the spectra. The spectrum for a Poisson process would hover about the dotted horizontal line, with minor variations. This dotted line represents λ, which is equal to the mean firing rate for the process. Temporal structure in the process would be evidenced by significant deviations from this value. However, the gray lines in the figure are representative of a 95% confidence interval and enclose the value of λ throughout the spectrum. It is also worthwhile to note that the spectrum is significantly lower than the mean at low frequencies, though this is consistent with the idea that the probability of a spike is reduced immediately following a prior spike (Jarvis and Mitra, 2001). Two frequency bands are also highlighted in the spectra – in the darker gray is the low frequency band, 0-10 Hz, and in the lighter gray is the gamma band, 30-100 Hz. Comparisons of mean normalized

spectral value between visual conditions within each frequency band were made using a permutation test with 1000 resamples. For the example neuron shown, significant difference was found for both low-frequency and gamma bands between vision and nonvision conditions.

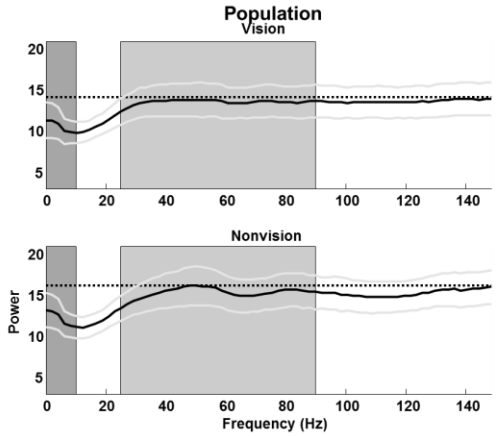

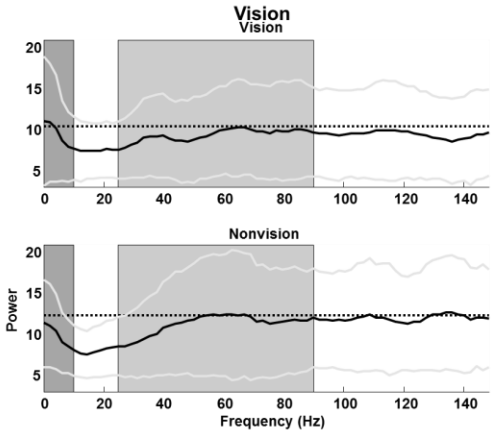

Figure 6 (left) Population spectra for all cells with at least one significant effect (main or interaction) in the ANOVA. Plot conventions as in Figure 5.
Figure 7 (right) Population spectra for all cells with significant main effect of vision. Plot conventions as in Figure 5.

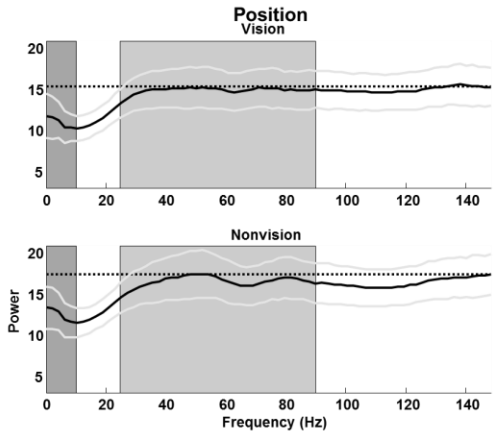

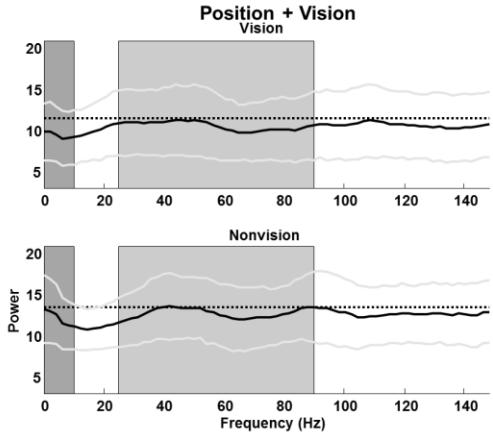

Figure 8 (left) Population spectra for all cells with significant main effect of position. Plot conventions as in Figure 5.
Figure 9 (right) Population spectra for all cells with significant interaction effect of position and vision. Plot conventions as in Figure 5.

Figure 6 shows population spectra for all cells with responses to at least one main effect or interaction. These population spectra were constructed using a bootstrap mean and confidence interval with 1000 resamples of the calculated spectra for the responsive cells.

Similar to the individual neuron in Figure 5, the neuron does not show significant deviation from λ. Comparisons of mean normalized spectral values between conditions within frequency bands showed no significant difference between conditions in either frequency band.

Figures 7-9 show population spectra for cells with significant main effects of vision (Fig. 7), position (Fig. 8), or an interaction of position and vision (Fig. 9). For all spectra in both conditions, no significant deviations from λ are seen, excepting the suppression at low frequencies consistent with the refractory period of a neuron. Comparisons of mean normalized spectral values showed that cells with both main effects showed differences between conditions in the gamma band (30-100 Hz) but not in the low frequency band (0-10 Hz) (Table 1). Cells with the position/vision interaction effects showed a significant difference between conditions in the gamma band and also in the low frequency band. Cells with main effects of vision or position did not show significant difference in the 0-10 Hz range. Differences can also be seen in Table 1.

Table 1: Significant Differences between V and NV conditions for population, main and interaction effects and different frequency bands.

	Vision	Position	Interaction
0-10 Hz	-	-	*
30-100 Hz	*	*	*

Chapter 4

DISCUSSION

The aim of this study was to assess the temporal structure in neural spiking activity in area 5 of the parietal cortex and to assess differences in neural behavior in conditions with and without visual feedback provided. Spectral analysis of the population responses showed that there was no significant temporal structure that deviated from the structure of a homogeneous Poisson process (i.e. flat at value λ, the mean firing rate), excepting a small amount of suppression at low frequencies, consistent with the existence of a refractory period where spike probability is reduced immediately following a spike. However, it was noted that differences in normalized spectral power occurred in the gamma band (30-100 Hz) for cells with significant main effect of vision condition, limb position, and/or interaction effect. These differences are suggestive of unique temporal spiking patterns at the individual level that may be influential at the population level.

In attempting to understand the way that neural spiking behavior can encode information, there are two main features of a spike train that can be decoded: mean and variance (Pesaran, 2002). It is well known that mean firing rate of a neuron can be used to indicate the responsiveness of a neuron (or population of neurons) to a given stimulus, but it is recently becoming clear that the variance of the spiking pattern can also be used to encode information about the response to the stimulus (Churchland et al., 2010). The frequency spectrum of a signal is an important tool in assessing the temporal structure of a signal that can contribute to sources of variability within the signal. Reverberations in a neural signal are thought to be important in cognitive processing of neural information (Pesaran, 2002). Temporal structure – characterized by peaks in the spectrum at frequencies with

concentrated power – could potentially be used along with mean rate information by other brain areas to give task-relevant activity such as the direction of a planned reach or other movement (Buneo, 2003).

Two other statistical tools that can be used to measure the variability are the Fano factor (FF) and coefficient of variation (CV), which are measures of variance normalized by the mean. In studying neural data, FF is used with the spike count for a trial, and as such, measures trial-by-trial variability in neural response to a stimulus. It has been shown that FF decreases with stimulus onset, suggesting that neural systems stabilize when being driven (Churchland, 2010). The previous analysis, in which it was found that the FF was lower in trials where vision was provided than in trials where vision was withheld, was consistent with this idea. The CV uses the inter-spike interval for a neuron and so measures the intra-trial variability of the signal. In previous analysis, it found that the CV was also lower in trials with vision than in trials without, suggesting a difference in intra-trial variability between the two conditions. In order to further probe the source of these differences in intra-trial variability, I employed spectral analysis to analyze the temporal structure of the signals in each condition, to see if differences there could account for the differences in the CV.

Peaks in the spectrum can be been indicative of enhanced rhythmicity, creating oscillations that may be read out by other brain areas (Buneo, 2003). However, this behavior was not seen in area 5. While spectral analysis did not yield significant differences in temporal structure, differences in mean normalized power were observed in the gamma band for cells with responses to each effect (main and interaction effects). These results imply that maintenance of static limb position in the presence or absence of visual feedback is associated with unique temporal patterns of spiking in the parietal cortex. The differences in these patterns of spike timing do not appear to be associated with a unique temporal

structure. This is consistent with the findings of Joelving et al. (2007), who found that rhythmic neuronal firing at the single neuron level is not a characteristic of active maintenance of visuospatial information in memory in area 7 of the parietal cortex. The authors also noted that while oscillatory activity may not be apparent at the single cell level, a sufficiently large population may be able to exhibit rhythmic activity, if individual neurons lock in to the oscillations at different times.

In order to gain deeper insight into activity in area 5, future work may include analysis of local field potential (LFP) data. It has been shown that spiking behavior and LFPs are coherent in the lateral intraparietal area in the gamma frequency band (Pesaran, 2002), making this a promising avenue to understanding neural behavior in area 5. Understanding the relationship between spiking behavior and LFP can help bridge the gap between single-neuron and population activity (Joelving et al., 2007). In continuing to study the behavior of area 5, it is possible to further advance the understanding of multimodal representation of limb position in the brain, an important step in the development of neural prosthetics.

REFERENCES

Buneo, C. A., Jarvis, M. R., Batista, A. P., & Andersen, R. A. (2003). Properties of spike train spectra in two parietal reach areas. *Experimental brain research*, *153*(2), 134-139.

Churchland, M. M., Byron, M. Y., Cunningham, J. P., Sugrue, L. P., Cohen, M. R., Corrado, G. S., ... & Shenoy, K. V. (2010). Stimulus onset quenches neural variability: a widespread cortical phenomenon. *Nature neuroscience*, *13*(3), 369-378.

Durand, D. M. (2006). What is neural engineering?. *Journal of Neural Engineering*, *4*(4).

Eisen, M. D. (2003). Djourno, Eyries, and the first implanted electrical neural stimulator to restore hearing. *Otology & neurotology*, *24*(3), 500-506.

Green, A. M., & Kalaska, J. F. (2011). Learning to move machines with the mind. *Trends in neurosciences*, *34*(2), 61-75.

Hochberg, L. R., Serruya, M. D., Friehs, G. M., Mukand, J. A., Saleh, M., Caplan, A. H., ... & Donoghue, J. P. (2006). Neuronal ensemble control of prosthetic devices by a human with tetraplegia. *Nature*, *442*(7099), 164-171.

Jarvis, M. R., & Mitra, P. P. (2001). Sampling properties of the spectrum and coherency of sequences of action potentials. *Neural Computation*, *13*(4), 717-749.

Joelving, F. C., Compte, A., & Constantinidis, C. (2007). Temporal properties of posterior parietal neuron discharges during working memory and passive viewing. *Journal of neurophysiology*, *97*(3), 2254-2266.

Li, Y., Smith, L.H, Hargrove, L.J., Weber, D.J., Loeb, G.E. (2013). Sparse Optimal Motor Estimation (SOME) for Extracting Motor Commands for Prosthetic Limbs. *IEEE Transactions on Neural Systems and Rehabilitation Engineering*, *21*(1), 104-111.

Maor, E. (2002). *Trigonometric delights*. Princeton University Press.

Nawrot, M. P., Boucsein, C., Rodriguez Molina, V., Riehle, A., Aertsen, A., & Rotter, S. (2008). Measurement of variability dynamics in cortical spike trains.*Journal of neuroscience methods*, *169*(2), 374-390.

Nicolelis, M. A. (2003). Brain–machine interfaces to restore motor function and probe neural circuits. *Nature Reviews Neuroscience*, *4*(5), 417-422.

Percival, D. B., & Walden, A. T. (1993). *Spectral analysis for physical applications*. Cambridge University Press.

Pesaran, B., Pezaris, J. S., Sahani, M., Mitra, P. P., & Andersen, R. A. (2002). Temporal structure in neuronal activity during working memory in macaque parietal cortex. *nature neuroscience*, *5*(8), 805.

Polikov, V. S., Tresco, P. A., & Reichert, W. M. (2005). Response of brain tissue to chronically implanted neural electrodes. *Journal of neuroscience methods*, *148*(1), 1-18.

Schwartz, A. B., Cui, X. T., Weber, D. J., & Moran, D. W. (2006). Brain-controlled interfaces: movement restoration with neural prosthetics. *Neuron*,*52*(1), 205-220.

Shi, Y., Apker, G.A., Buneo, C.A. (2013) Multimodal representation of limb endpoint position in the posterior parietal cortex. *Journal of* Neurophysiology, *109,* 2097-2107.

APPENDIX A

IACUC APPROVAL FORM

Institutional Animal Care and Use Committee (IACUC)
Office of Research Integrity and Assurance
Arizona State University
660 South Mill Avenue, Suite 315
Tempe, Arizona 85287-6111
Phone: (480) 965-4387 *FAX:* (480) 965-7772

Animal Protocol Review

ASU Protocol Number:	**12-1260R**
Protocol Title:	**Cortical Mechanisms of Sensorimotor Integration**
Principal Investigator:	**Christopher Buneo**
Date of Action:	**5/31/2012**

The animal protocol review was considered by the Committee and the following decisions were made:

- ☐ The original protocol was APPROVED as presented.
- ☒ The revised protocol was APPROVED as presented.
- ☐ The protocol was APPROVED with RESTRICTIONS or CHANGES as noted below. The project can only be pursued, subject to your acceptance of these restriction or changes. If you are not agreeable, contact the IACUC Chairperson immediately.
- ☐ The Committee requests CLARIFICATIONS or CHANGES in the protocol as described in the attached memorandum. The protocol will be considered when these issues are clarified and the revised protocol is submitted.
- ☐ The protocol was approved, subject to the approval of a WAIVER of provisions of NIH policy as noted below. Waivers require written approval from the granting agencies.
- ☐ The protocol was DISAPPROVED for reasons outlined in the attached memorandum.
- ☐ The Committee requests you to contact _____ to discuss this proposal.
- ☐ A copy of this correspondence has been sent to the Vice President for Research.
- ☐ Amendment was approved as presented.

Documentation of Level III Training will need to be provided to the IACUC office before the participant can perform procedures independently. For more information on Level III requirements see https://researchintegrity.asu.edu/training/animals/levelthree

Total # of Animals:	**9**	**Pain Level:**	**D**	**Species:**	**Macaca mulatta**
Sponsor:	**NSF**				
Proposal/Award #:	**020563-001**				
Title:	**Characterizing Neural Mechanisms of State Estimation in the Posterior Parietal Cortex**				
Approval Period:	**5/31/2012 – 5/30/2015**				

Signature: C. Miller for D. Murphy Date: 5/31/12
IACUC Chair or Designee

Original: Principal Investigator
Cc: IACUC Office
IACUC Chair